An Energy-Efficient Reliable Data Transmission Scheme for Complex Environmental Monitoring in Underwater Acoustic Sensor Networks

Kun Wang, *Member, IEEE*, Hui Gao, Xiaoling Xu, Jinfang Jiang, *Member, IEEE*, and Dong Yue, *Senior Member, IEEE*

***Abstract*— As an extension of wireless sensor network in underwater environment, underwater acoustic sensor networks (UASNs) have caused widespread concern of academia. In UASNs, the efficiency and reliability of data transmission are very challenging due to the complex underwater environment in variety of ocean applications, such as monitoring abnormal submarine oil pipelines. Motivated by the importance of energy consumption in many deployments of UASNs, we therefore propose an energy-efficient data transmission scheme in this paper, called energy-efficiency grid routing based on 3D cubes (EGRCs) in UASNs, considering the complex properties of underwater medium, such as 3D changing topology, high propagation delay, node mobility and density, as well as rotation mechanism of cluster-head nodes. First, the whole network model is regarded as a 3D cube from the grid point of view, and this 3D cube is divided into many small cubes, where a cube is seen as a cluster. In the 3D cube, all the sensor nodes are duty-cycled in the media access control layer. Second, in order to make energy efficient and extend network lifetime, the EGRC shapes an energy consumption model considering residual energy and location of sensor nodes to select the optimal cluster-heads. Moreover, the EGRC utilizes residual energy, locations, and end-to-end delay for searching for the next-hop node to maintain the reliability of data transmission. Simulation validations of the proposed algorithm are carried out to show the effectiveness of EGRC, which performs better than the representative algorithms in terms of energy efficiency, reliability, and end-to-end delay.**

***Index Terms*— Data transmission, energy efficiency, routing, underwater acoustic sensor networks (UASN), environmental monitoring.**

Manuscript received March 1, 2015; revised April 23, 2015; accepted April 23, 2015. Date of publication May 5, 2016; date of current version April 26, 2016. This work was supported in part by the National Natural Science Foundation of Jiangsu Province under Grant BK20141427, in part by the National Natural Science Foundation of China under Grant 61100213, Grant 61170276, and Grant 61401107, in part by the SFDPH under Grant 20113223120007, in part by the Huawei Innovation Research Program under Grant YB2014010048, in part by the Nanjing University of Posts and Telecommunications under Grant NY214097 and Grant XJKY14011, in part by the Educational Commission of Guangdong Province under Grant 2013KJCX0131, and in part by the Guangdong High-Tech Development Fund under Grant 2013B010401035. The associate editor coordinating the review of this paper and approving it for publication was Dr. J. J. P. C. Rodrigues.

K. Wang, H. Gao, and D. Yue are with the Institute of Advanced Technology, Nanjing University of Posts and Telecommunications, Nanjing 210003, China (e-mail: kwang@njupt.edu.cn; wdxhg6@163.com; medongy@vip.163.com).

X. Xu is with the Guangdong University of Petrochemical Technology, Guangdong 525000, China (e-mail: xiaoling.xu2015@outlook.com).

J. Jiang is with the Department of Information and Communication Engineering, Hohai University, Changzhou 213022, China (e-mail: jiangjinfang1989@gmail.com).

Digital Object Identifier 10.1109/JSEN.2015.2428712

I. Introduction

IN ORDER to better research and develop marine resources, modern communication systems and networks have extended from the land and air to the ocean. Underwater Acoustic Sensor Networks (UASNs), which plays an important role in the marine resources exploration and development, integrated ocean environmental monitoring and other related systems [1], especially in monitoring abnormal submarine oil pipelines, has developed rapidly in recent years. With the lack of terrestrial oil resources, oil exploring and transmission have dabbled in ocean. However, oil leaking may pollute the marine environment, which is a terrible threat to marine life and mankind. Therefore, abnormal monitoring of marine oil pipelines in case of leaking is vital indeed.

Accordingly, researches on USANs provide the technique guarantee for information transmission underwater. What's more, UASNs have been used widely in many applications where sensor nodes collaborate with each other to execute monitoring tasks with reliability and energy-efficiency [2].

There are many similarities but also differences between UASNs and Terrestrial Wireless Sensor Networks (TWSNs) [3], which are all important fields in wireless sensor networks:

1) In the aspect of communication mode, traditional TWSNs use radio signal, while UASNs use underwater acoustic channel to transmit data. That's because radio signal attenuates seriously in the underwater environment, and only achieves high-speed transmission in short, which cannot reach the requirements of long-distance underwater communication. Therefore, radio signal is not suitable for underwater acoustic sensor networks. However, there are drawbacks in underwater acoustic channel, such as high end-to-end delay, low bandwidth and high bit error rate.

2) In the aspect of network characteristics, the network model of TWSNs is basically two-dimensional, while the network model of UASNs can be seen as three dimensions since nodes are deployed in the ocean. Meanwhile, the deployment of nodes in USANs meets more difficulties due to the limitations of underwater environment and costs.

3) In the aspect of energy consumption, sensor nodes carry limited batteries both in UASNs and TWSNs. However, the nodes in TWSNs can be replaced at any time, but the modems of UASNs can hardly be changed. Since the nodes in UASNs are underwater, node replacement needs long time

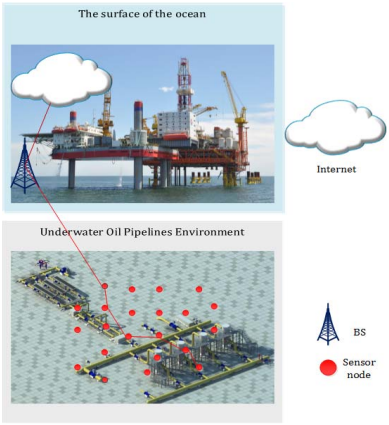

Fig. 1. Marine monitoring scenario based on UASNs.

sailing, much resource consumption and high costs. Moreover, in consideration of the complex environment of ocean and widespread of sensor nodes, it is unrealistic to recharge the energy of nodes by changing batteries.

Therefore, existing routing protocols in TWSNs cannot directly be applied to UASNs. Additionally, in consideration of the high power of underwater acoustic modems and the difficulties in changing sensor nodes because of the harsh environment, the energy efficiency in UASN is even more vital [4].

Problem Statement: Fig. 1 is a classic application scenario for marine oil pipeline monitoring. In this figure, many sensor nodes are deployed randomly in the ocean where oil pipelines are distributed all around. Nodes collect useful abnormal monitoring information of local scene, and send information to BS for analyzing the leaking of oil pipelines. In this paper, we are extremely interested in seeking a proper energy-efficient data transmission scheme in duty-cycle based UASNs for this kind of monitoring applications. Particularly, our interests fall into the following two aspects:

- Will multi-hop, duty-cycle and an energy-efficiency protocol be integrated for reliable underwater data transmission in monitoring applications?
- Will 3D Geospatial Division as well as other complex properties (such as three dimensional changing topology, high propagation delay, node mobility and density) of underwater medium be considered in UASNs?

To this end, An EGRC (Energy-efficiency Grid Routing based on 3D Cubes) in UASNs is proposed. First, the whole network, which can be viewed as a big cube, is divided into some SCs (Small Cubes), where a SC is a cluster. Second, we propose a novel approach to select the cluster-head node, namely, choosing a node in SC with the highest residual energy and the shortest distance to BS to take charge of data aggregation and transmission in SC. Finally, we adopt a data transmission mechanism with a combination of single hop and multihop, in which multihop routing also takes the residual energy, relative distance and end-to-end delay into account. Simulations show that this EGRC is characterized by energy efficiency, low latency and reliability with long network lifetime.

The rest of the paper is organized as follows. In Section II, we give the related literatures from three aspects. The detailed operations of EGRC is presented in Section III. Section IV shows the performance evaluation of EGRC and comparison with related algorithms. Finally, we draw the main conclusions in Section V.

II. Related Work

In this section, we present the existing literatures on clustering, grid routing protocols and energy-efficiency schedule. Then the novelty of our work is concluded.

A. Clustering Protocols

Clustering issues and algorithms have been widely investigated in TWSNs [5]–[8]. However, those protocols cannot be directly applied in UASNs. Ayaz *et al.* [9] proposed a mobility-aware routing protocol, called Temporary Cluster Based Routing (TCBR), which does not require any location information of nodes, and only a small number of nodes are involved during the end-to-end routing process. Domingo and Prior [10] presented a Distributed Underwater Clustering Scheme (DUCS), a new GPS-free routing protocol for Underwater Sensor Networks (UWSNs). This scheme does not use flooding techniques, minimizing proactive routing message exchange. Ovaliadis *et al.* [11] proposed an improved cluster system against cluster-head failures, suggesting that a primary cluster-head and a backup cluster-head are selected in network. Goyal *et al.* [12] designed a fuzzy-based clustering and aggregation technique for UASNs, which selects cluster-head node with fuzzy logic module, where the input parameters of this fuzzy logic are residual energy, distance to sink, node density, load and link quality.

B. Grid Routing Protocols

Han *et al.* [13] presented a novel KNN (k-Nearest Neighbor algorithm) query algorithm based on grid division routing in the setting of skewness distribution, where the connectivity of adjacent grid centers forms the itinerary. Chi and Chang [14] proposed an energy-aware grid-based routing scheme for WSNs to save energy with mobile observations. Kim *et al.* [15] presented a routing protocol based on hex-grid in WSNs, which can reduce energy consumption with Hex-grid to find paths. All the algorithms above are based on grids in TWSNs, but there are few algorithms based on cubes in UASNs because of three-dimension. Ren *et al.* [16] proposed a novel cube-scan-based three dimensional multi-hop localization algorithm for large-scale UWSNs, suitable for large-scale UASNs with limited computing power and energy, in which the node coordinates are obtained through a cube-scan procedure to constraint the relationship between nodes.

C. Energy-Efficiency Schedule

Some routing protocols were proposed to reduce energy consumption in TWSNs [17]–[20]. Similarly, UASNs also need schedules to balance energy consumption. Ali *et al.* [21] proposed a novel routing protocol called

Layer by layer Angle-Based Flooding (L2-ABF) to address the issues of continuous node movements, end-to-end delay and energy consumption, in which every node can calculate its flooding angle to forward data packets to the sinks without using any explicit configuration or location information in this routing protocol. Zhang *et al.* [22] proposed a link detection mechanism to get link state information (symmetrical link or asymmetric link), and adopted an adaptive routing feedback approach to make full use of the underwater asymmetric link and save energy. Besides, a downstream node table and a time-based priority forwarding mechanism are utilized to prevent flooding, and a credit-based routing table update mechanism is adopted to avoid energy consumption caused by frequent update of routing table. Gopi *et al.* [23] proposed an Energy optimized Path Unaware Layered Routing Protocol (E-PULRP) for dense 3D UWSNs, in which sensor nodes report events to a sink node using on-the-fly routing to save energy. A hybrid data transmission mechanism based on energy level was proposed to balance energy consumption in [24], where an optimal classification number of energy level is evaluated through theoretical analysis in this mechanism.

D. The Contributions of Our Work

Compared with the above-mentioned related works, the contributions of our paper can be listed as follows:

- This paper focuses on integrating multiple techniques for underwater data transmission. A 3D big cube is provided with integration of multi-hop, duty-cycle and a proper energy-efficiency protocol altogether in network model. A kind of data transmission schemes, i.e., Energy-efficiency grid routing scheme (EGRC) is come up with based on 3D cubes, which can be applied in underwater circumstances.
- This paper also focuses on 3D Geospatial Division as well as other complex properties of underwater medium in UASNs. Since the 3D underwater network is divided into small cubes, data packets are collaboratively transmitted as units of small cube spaces logically, while in fact data packets are still transmitted between sensor nodes in both single-hop and multi-hop mode. In this 3D big cube (BC), several SCs with fixed size are divided to form different clusters. Node density varies with the changing of SC's size.
- In EGRC, a novel approach to select cluster-head node is proposed based on energy consumption. A node with high energy and short distance to base station is selected as cluster-head node in charge of data aggregation and transmission of this SC. What's more, a rotation mechanism of cluster-head node is introduced where nodes in a SC take turns to be selected as the cluster-head node when data packets are transmitted in a timer period. Meanwhile, an effective searching algorithm is adopted to search for the next-hop using energy, distance and end-to-end delay as parameters. EGRC ultimately saves nodes' energy consumption, improves data transmission efficiency and network reliability.

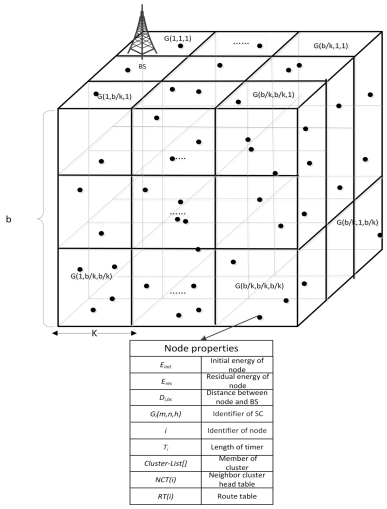

Fig. 2. Network model.

III. ENERGY-EFFICIENT DATA TRANSMISSION SCHEME

In this section, we first setup the network model,energy consumption model with 3D cube introduction and delay model. Then, cluster-head node selection, next-hop node selection and data transmission procedure are described with specific example in detail.

A. Network Model

To facilitate our research, we have the following assumptions:

1) 3D underwater network is set and divided into SCs. Data packets are collaboratively transmitted as units of SC spaces logically, while in fact data packets are still transmitted between sensor nodes in both single-hop and multi-hop mode. Node density varies with the changing of SC's size.
2) The number of sensor nodes is N. Base station node is on the surface of monitoring area. Sensor nodes are deployed in monitoring area randomly. Positioning algorithms [25] can be used to obtain the geographical coordinates of its own and base station.
3) Each sensor node has its unique identifier and the same initial energy, transmission power and communication range. Energy can be provided constantly to base station. Energy consumption for nodes to aggregate data is E_{da}(n J/bit/packet).
4) BS and the whole BC are fixed. All nodes move randomly at the same speed and are duty-cycled in this BC. Nodes do not care of stepping into other SCs because of cluster-head node reselection. All nodes in a SC are able to take turns to be selected as the cluster-head node when data packets are transmitted in a timer period.

1) 3D Geospatial Division: We set up UASN scenario in a 3D-environment [26]. Therefore, we can model a 3D UASN as a Big Cube (BC). The top surface of BC refers to the surface of the water and the bottom one refers to the seabed, as shown in Fig. 2. The length of BC's edge is b. BS with both acoustic and radio modems is located on the water surface,

i.e., the coordinates of vertex for the top right corner of BC is (0, 0, 0). BC is carefully divided into SCs in a multi-magic cube manner. The length of SC's edge k is related to the communication range of node c.[1] The number of sensor nodes in one SC is determined by node density. Each SC is numbered as $G_i(m,n,h)$, where m, n, h=1,2,...,$\frac{b}{k}$. For each node $i(x,y,z)$, its SC identifier $G_i(m,n,h)$ can be calculated by equations (1, 2, 3), where m, n, and h appear to be smaller when node gets closer to BS. When the network configuration is completed, BS broadcasts the length of SC's edge k and the coordinates of BS to all the nodes. According to equation (4), each node calculates the distance $D_{i,bs}$ between node and BS by its own coordinates (x,y,z). Then node gets to know which SC the node is located in with the value (m,n,h), and marks a SC.

$$m = \frac{k - x \ mod \ k + x}{k} \tag{1}$$

$$n = \frac{k - y \ mod \ k + y}{k} \tag{2}$$

$$h = \frac{k - |z| \ mod \ k + |z|}{k} \tag{3}$$

$$D_{i,j} = \sqrt{(x_i - x_j)^2 + (y_i - y_j)^2 + (z_i - z_j)^2} \tag{4}$$

2) Information Storage: Nodes in one SC select the cluster-head node with our proposed algorithm (described in Cluster-head Selection), and send the collected nodes' information[2] to cluster-head node. After sending the data, nodes recalculate the value *(m, n, h)*, mark a new SC, and reselect cluster-head node of this new SC. Cluster-head node has the information of all nodes in local SC which is stored in *Cluster-List []*.

3) Duty-Cycled Rule: As for cluster-head node, each SC selects its own cluster-head node. This cluster-head node takes charge of information of all the nodes in SC, and is responsible for aggregating the data that nodes in SC collect, selecting the best route to BS and transmitting data as a relay node. The cluster-head node selects other nodes in SC to collect information according to the residual energy of nodes. When a cluster-head node aggregates or transmits data packets, other nodes go into sleep mode [27], [28]. This connected K-Neighborhood sleep scheduling algorithm (CKN) aims at allowing a part of sensor nodes go to sleep while at least K of those nodes' neighbor awake to keep those nodes all K-connected. Therefore, the number of sleeping nodes in our algorithm can be adjusted when changing the value of K.

B. Energy Consumption Model

An energy consumption model with free space and multi-path transmission which is similar to LEACH [29] is adopted in TWSN. Energy consumption of nodes is mainly composed of energy consumption for communication and data processing, in which, energy consumption for data transmission is related to communication environment, transmission distance and packet size. Generally, energy consumption for a node to transmit bit data packets to another node is set as equation (5):

$$E_{tx} = \begin{cases} l\varepsilon_{elec} + l\varepsilon_{fs}d^2, & d < d_0 \\ l\varepsilon_{elec} + l\varepsilon_{mp}d^4 & d \geq d_0 \end{cases} \tag{5}$$

where l is the number of bits of one packet, d is distance between transmitter and receiver, d_0 is a threshold distance to transmit data packets, ε_{elec} is the radio dissipation of running transmitter and receiver circuitry, and ε_{fs} and ε_{mp} represent transmit amplifier coefficient of free space and multipath model, respectively. If $d < d_0$, the amplifier coefficient of free space model $\varepsilon_{fs}d^2$ is adopted. Otherwise, the amplifier coefficient of free multipath model $\varepsilon_{mp}d^4$ is adopted.

However, considering the differences between TWSN and UASN of communication mode, the signal amplifier energy is also different between radio signal and acoustic signal. In UASN, no matter the free space module or multipath model, the amplifier coefficient is defined as $a(f)^d$ [30], where $a(f)$ is the absorption coefficient, d is the distance between transmitter and receiver, and f is the frequency of acoustic signal. What's more, $a(f)$ can be expressed empirically using the Thorps formula. For frequency 1000 Hz, there holds [31]

$$\log a(f) = 0.011\frac{f^2}{1+f^2} + 4.4\frac{f^2}{4100+f^2} + 2.75 \times 10^{-5} f^2 + 0.0003 \tag{6}$$

Therefore, we have the definition for the energy consumption:

Definition 1: The energy consumption for a node to transmit l bits data packets to another node where the distance between the two nodes is d with the frequency f is modified as:

$$E_{tx} = \begin{cases} l\varepsilon_{elec} + la(f)^d d^2, & d < d_0 \\ l\varepsilon_{elec} + la(f)^d d^4 & d \geq d_0 \end{cases} \tag{7}$$

Definition 2: Energy consumption for node to receive bit data packets is defined as follows:

$$E_{Rx} = l\varepsilon_{elec} \tag{8}$$

In addition, we assume information that a node in a SC collects is highly correlated. Therefore, cluster-head nodes can aggregate information collected by cluster members into a single packet. However, information collected in different SCs has a low degree of correlation. As a result, nodes between cluster-head node and BS would not aggregate the data packets it transmits.

C. Delay Model

When a packet is sent from the source node to any destination, there is an end-to-end delay. In normal conditions, the end-to-end delay consists of the following types [32]:

1) Transmission and reception time: The delay of sending or receiving the whole packet over the channel. It is the function of packet size and data transmission rate.

2) Propagation time: The time for a signal traversing from a source node to the receiver. This is related with the speed of acoustic signal in water.

[1] In order to communicate with the cluster-head node in adjacent SC, the length of diagonal line of two SCs (the longest distance between this SC and adjacent SC) must be equal or smaller than c.

[2] Here nodes' information includes node identifier, coordinate of node, SC identifier, Residual energy, Distance to BS, etc.

3) Byte alignment time: The time that packet waits at the routing queues. It is determined by the congestion situation of the network.

Then we denote the transmission and reception time of node i by tr_i, the propagation time from node i to j by pr_{ij}, and the byte alignment time of node i by a_i. Therefore, the delay t_{ij} from node i to j can be calculated as the following equation:

$$t_{ij} = tr_i + pr_{ij} + a_i \tag{9}$$

As the transmission and reception time tr_i is the function of packet size p and data transmission rate r_i of node i, then

$$tr_i = \frac{p}{r_i} \tag{10}$$

Whats more, the propagation time pr_{ij} from node i to j is related to the distance D_{ij} between node i to i and the speed of acoustic signal v_{sound} in water, so

$$pr_{ij} = \frac{D_{i,j}}{v_{sound}} \tag{11}$$

In addition, we define the end-to-end delay should be less than the delay threshold t_{th} in this paper.

D. Cluster-Head Selection

Cluster-head selection in most clustering routing protocols for WSNs is composed of two phases, i.e., selecting cluster-head node and forming a cluster. In this paper, however, the whole network is divided into several SCs, and these SCs are regarded as a clusters. As a result, the selection of cluster-head node can be accomplished in a SC.

After a node receives a *Cube-length* message broadcasted by BS, it calculates SC identifier, and the phase of cluster-head selection starts as follows:

1) Node calculates its own SC identifier $G_i(m,n,h)$ according to k in *Cube-length* message, and starts a timer when the network deploys, and sets $Cluster_T$ to 1. What's more, node will start the timer when it sends data to cluster-head node or BS. T_i is determined by equation (12, 13):

$$T_i = T_{max} \cdot \frac{E_{res}}{E_{init}} \cdot \frac{D_{G,bs} - D_{i,bs}}{D_{G,bs}} \tag{12}$$

$$D_{G,bs} = k\sqrt{(m^2 + n^2 + h^2)} \tag{13}$$

where E_{res} is the residual energy, E_{init} is the initial energy of node, $D_{G,bs}$ is the maximum distance from SC to BS and $D_{i,bs}$ is distance between node to BS. Since initial energy is constant, the more residual energy is and the closer to BS, the smaller T_i is. Accordingly, the less residual energy is, the bigger T_i is and closer to T_{max}.

2) Node broadcasts *Cluster-Msg* message after the end of timer in the range of $\sqrt{3}k$[3]. *Cluster-Msg* includes node identifier, node coordinates (x,y,z), distance to BS $D_{i,bs}$, SC identifier $G_i(m,n,h)$ and the residual energy E_{res}.

3) If node receives *Cluster-Msg* message from other nodes before the end of timer, then it judges the information of *Cluster-Msg* message. If SC identifier in the message is the same as that of the node, an index to indicate the possibility of being a cluster-head node C_i is calculated according to equation (14) and does comparison.

$$C_i = \frac{E_{res}}{D_{i,bs}} \tag{14}$$

If C_i from the message (calculated by equation (14)) is bigger than its own C_i, the timer stops and an tag $Cluster_T$ is set to 0. Otherwise, this massage is saved to *Cluster-List []* and the timer continues to timing. Similarly, if SC identifier from the message is inconsistent with its own SC identifier, the message will be dropped and the timer continues to timing. Equation (14) indicates that the more the residual energy is and the closer the node to BS is, the more possibility this node i is selected as a cluster-head node.

4) If node receives *Cluster-Msg* message from other nodes after the timer is out, it judges whether the SC identifier is the same. If so and if the $Cluster_T$ of the information equals to 1, the tag $Cluster_T$ of this node is set to 0. Meanwhile, the node who sends *Cluster-Msg* message is set as a cluster-head node. Otherwise, the received message is abandoned. The pseudo-code of selecting a cluster-head node in a SC is given in ALGORITHM 1.

All nodes in a SCs are able to take turns to be selected as the cluster-head node when data packets are transmitted in a timer period.

As an example, the detailed procedure of cluster-head selection is shown in Fig. 3. In this figure, assuming that there

Algorithm 1 Cluster-Head Node Selection

Inputs:*Cube-length* message, residual energy of node E_{res}, distance between node i and BS $D_{i,bs}$, coordinates of node (x,y,z), SC identifier $G_i(m,n,h)$, length of timer T_i, node identifier i

Output: cluster-head node of SC

```
BEGIN
  start the timer T_i
  Cluster_T =1
  WHILE (T_i != 0) DO
    ReceiveCluMsg(j);
  //receive the Cluster-Msg message broadcasted by node j
before the end of timer
    IF (G_i(m,n,h) == G_j(m,n,h))
      C_i = E_res/D_i,bs; C_j = E_res/D_j,bs
  //calculate the value C and do comparison
      IF (C_i < C_j)
        Cluster_T =0
        T_i=0
      END IF
      ELSE
       Cluster-List [n]=j; n++;
  //add node j into Cluster-List[]
      END ELSE
    END IF
  END WHILE
  Broadcast();
  //broadcast Cluster-Msg message in the range of √3k;
   ReceiveCluMsg(j);
  //receive the Cluster-Msg message broadcasted
  by node j after the timer is out
  IF (G_i(m,n,h) == G_j(m,n,h))
    IF(Cluster_T (j)==1)
      Cluster_T =0;
      Cluster − head=j;
    ENDIF
  ENDIF
END
```

[3]It is noted that $\sqrt{3}k$ is set as the length of diagonal line in a SC for node to communicate with other nodes in local SC.

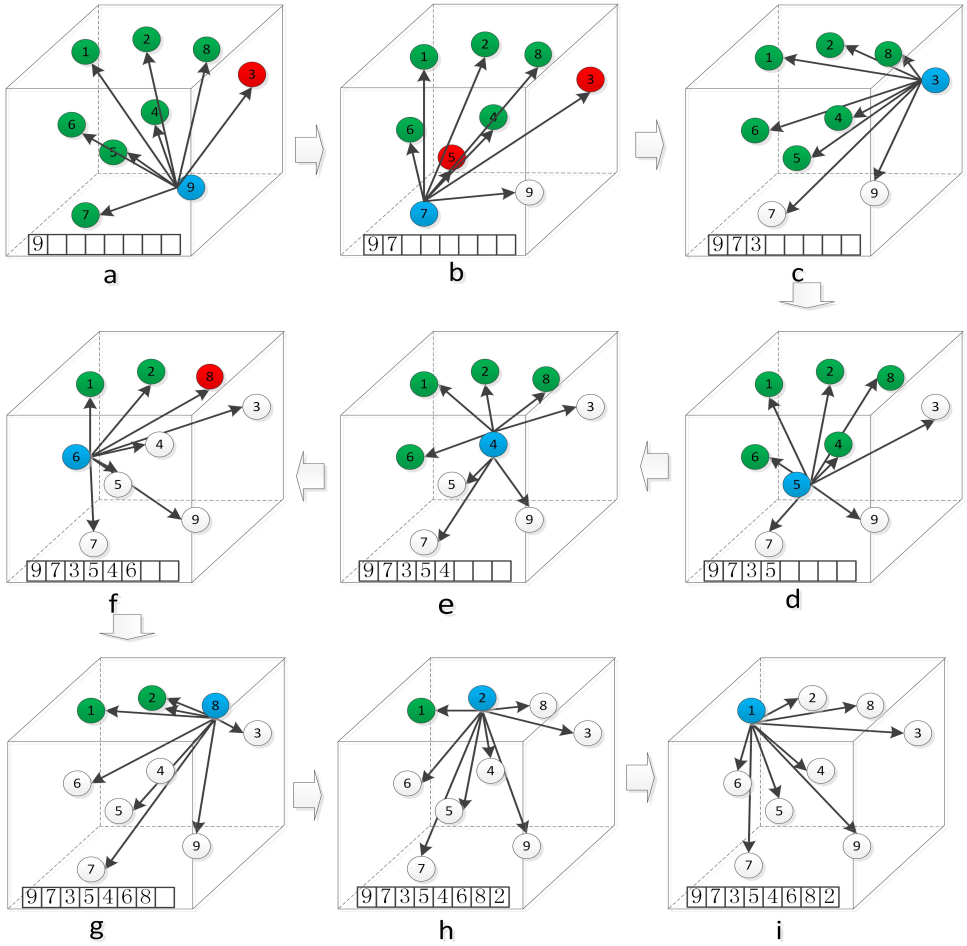

Fig. 3. (a) to (i) Procedure of cluster-head node selection.

are 9 nodes in this SC, where $T_1 > T_2 > T_8 > T_6 > T_4 > T_5 > T_3 > T_7 > T_9$ and $C_3 < C_9 < C_5 < C_7 < C_4 < C_8 < C_6 < C_2 < C_1$, we may select node 1 as the cluster-head node by the following steps. Firstly, the timer of node 9 runs out. Then node 9 broadcasts *Cluster-Msg* message to all the nodes. Nodes 1 to 9 compare the value C after receiving *Cluster-Msg* message. Since $C_3 < C_9 < C_5 < C_7 < C_4 < C_8 < C_6 < C_2 < C_1$, except node 3, all the nodes add node 9 to *Cluster-List[]* as shown in Fig. 3(a). Subsequently, node 1 will be selected as cluster-head node after 8 calculations and comparisons, as shown from Fig. 3(b) to (i).

After the procedure above, nodes in a SC form a cluster, and the node with the highest residual energy and shortest distance to BS is selected as a cluster-head node. Information of all the nodes in SC is stored in the *Cluster-List []* of this cluster-head node. Meanwhile, other nodes receive the message from cluster-head node about the information of cluster-head nodes. In addition, in order to obtain the information of cluster-head nodes with adjacent SCs, when a node is selected as a cluster-head node, it will broadcast *Cluster-Neighbor* message in a range of $\sqrt{6}k$,[4] including the residual energy of the cluster-head node E_{res}, SC identifier $G_x(m,n,h)$, the distance to BS $D_{x,bs}$, node coordinates (x,y,z) and cluster-head node identifier i. The node receiving *Cluster-Neighbor* message judges whether it is cluster-head node and whether the SC identifier is smaller than itself. If $Cluster_T$ is equal to 1 and the SC identifier is smaller than itself, nodes' information is stored in the message to NCT (Table I as an example). Otherwise, the message will be dropped.

[4]To communicate with the cluster-head node in adjacent SC for obtaining its information of NCT, here $\sqrt{6}k$ is set as the length of diagonal line of two SCs (the longest distance between this SC and adjacent SC).

TABLE I
NEIGHBOR CLUSTER TABLE

node identifier	Coordinate of node	SC identifier	Residual energy	Distance to BS
i	(x,y,z)	$G_x(m,n,h)$	E_{res}	$D_{x,bs}$
10	(8,15,17)	(2,4,5)	4852	17
22	(7,18,14)	(2,5,4)	4575	19.3

E. Data Transmission Mechanism

In clustering protocols, data transmission is usually divided into two phases, i.e., transmission from a normal node to cluster-head node and transmission from cluster-head node to BS.

In this mechanism, cluster-head nodes transmit data packets to BS by multihop. Meanwhile, another index *Vertex(i)* is set to indicate the possibility of being a next-hop node. First, cluster-head nodes in a $2k$-radius area around BS transmit data packets directly to BS by single hop. Second, other cluster-head nodes (here we take node c as an example) calculate the next-hop node as the following method. In order to save energy and extend network life as much as possible, we choose the minimum distance to BS, the minimum end-to-end delay to the source node and the maximum energy as next hop node. Therefore, the $next-hop\ finding\ problem(NFP)$ can be formulated as:

$$\begin{aligned} NFP: &for \min_{i\in NCT(c)} Vertex(i) \\ &= \min_{i\in NCT(c)} [\frac{D_{i,bs}}{D_{c,bs}} + \lambda(1-\frac{E_{res}(i)}{E_{res}(c)}) + \mu\frac{t_{i,c}}{t_{th}}] \\ &we\ want \min_{i\in NCT(c)} t_{i,c}, \min_{i\in NCT(c)} D_{c,bs} \\ &and \max_{i\in NCT(c)} E_{res}(i) \end{aligned} \tag{15}$$

where $D_{G,bs}$ is the distance between the SC that node c belongs to and BS; λ and μ are the parameters to value the importance of energy and delay. Therefore, we convert three performance metrics to a simple weight.

Due to the mobility of node in UASN, the location of node will change after sending the Cluster-Neighbor message, so the maximum moving distance after sending the message is $\frac{\sqrt{6k}}{v_{sound}}v$, then the weight above $Vertex(i)$ is adjusted to a range $[Vertex(i)-\Delta_{ic}^{-},\ Vertex(i)+\Delta_{ic}^{+}]$. where

$$\begin{aligned} \Delta_{ic}^{-} = &\frac{D_{i,bs} - \frac{\sqrt{6k}}{v_{sound}}v}{D_{G,bs}} + \lambda(1-\frac{E_{res}(i)}{E_{res}(c)}) \\ &+\mu\frac{t_{i,c} - \frac{\sqrt{6k}}{v_{sound}^2}v}{t_{th}} \end{aligned} \tag{16}$$

and

$$\begin{aligned} \Delta_{ic}^{+} = &\frac{D_{i,bs} + \frac{\sqrt{6k}}{v_{sound}}v}{D_{G,bs}} + \lambda(1-\frac{E_{res}(i)}{E_{res}(c)}) \\ &+\mu\frac{t_{i,c} + \frac{\sqrt{6k}}{v_{sound}^2}v}{t_{th}} \end{aligned} \tag{17}$$

mean the maximum decrement weight and increment weight, respectively.

In order to save energy, only cluster-heads whose grid number is smaller than $G_c(m,n,h)$ need to calculate the weight. Then, the node i in the Neighbor-List array with the smallest $Vertex(i)$ has the minimum lower bound in the range is chosen to be the next hop, and added to $RT(c)$ of cluster-head node c. Considering the overlapped part of node j with node i in the weight range, node j will also be added to $RT(c)$. Then, the cluster-head node c will route the data message with nodes in $RT(c)$. The pseudo-code of searching for next-hop node is given in Algorithm 2.

Algorithm 2 Searching for the Next-Hop Node

Inputs: Cresidual energy of cluster-head node $E_{res}(c)$, distance to BS $D_{c,bs}$, $NCT(c)$

Output: next-hop node

```
BEGIN
IF (D_{c,bs} < 2k)
    SendToBS(Data);
// send data to BS
ELSE
    FOR i ∈ NCT(c)
        Vertex(i) = D_{i,bs}/D_{c,bs} + λ(1 − E_res(i)/E_res(c)) + μ t_{i,c}/t_th
// node c calculates Vertex of every node
    END FOR
    MinVertex(Vertex(i));
// calculate the minimum of Vertex
    AddRouteTable(i);
// add the node with minimum Vertex into RT(c)
        FOR j ∈ NCT(c)
            IF (Vertex(j) + Δ_jc^− < Vertex(i) + Δ_ic^+)
//whether node j has the overlapped part with node i
//who has the minimum Vertex
                AddRouteTable(j);
// add node j into RT(c)
            END IF
        END FOR
    END ELSE
END
```

Fig. 4 shows the procedures when node A transmits data to BS as an example. In the figure, we assume that node B is the cluster-head node in node A's SC. Node C, D, E, F, G are cluster-head nodes of adjacent SCs, where $Vertex(E) < Vertex(C) < Vertex(F) < Vertex(D) < Vertex(G)$. After the selection of cluster-head node, node C,D,E,F,G broadcast *Cluster-Neighbor* message including residual energy E_{res}, SC identifier $G_x(m,n,h)$, distance to BS $D_{x,bs}$, node coordinates (x,y,z) and cluster-head node identifier i in the range of $\sqrt{5}k$. Meanwhile, node B receives *Cluster-Neighbor* messages from adjacent cluster-head nodes, and then calculates $Vertex$ by equation (10) according to *Cluster-Neighbor* messages. Since $Vertex(E) < Vertex(C) < Vertex(F) < Vertex(D) < Vertex(G)$, node B choose node G as the next-hop node. All the next-hop nodes are selected according to the steps above.

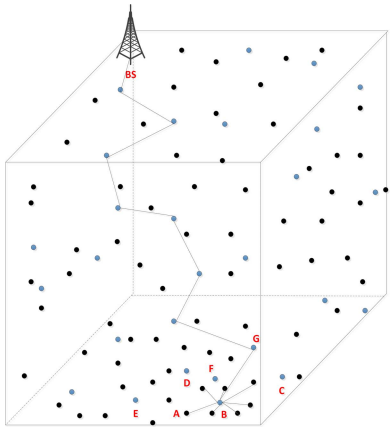

Fig. 4. Procedure of cluster-head node selection (the blue nodes are selected as the cluster-head nodes to transmit data packets as an example, and the black nodes are duty-cycled nodes in sleep mode).

IV. Performance Evaluations

In this section, the performance of EGRC is verified through three parts' simulations. In the first part, scene parameters change to select the optimal range of communication.

TABLE II
SIMULATION SETTINGS

Scene Parameter	Network scale	500m*500m*500m
	Location of BS	(0,0,0)
	Number of nodes	100, 200, ..., 600
	Simulation rounds	10, 20, ..., 400
	Compared algorithms	LEACH, EL-LEACH, ERP^{2}R VBF and L2-ABF
	k	10 m, 20 m, ..., 50 m
	c	50 m, 60 m, ..., 100 m
Node Parameters	E_{init}	2J
	ε_{elec}	50nJ/bit
	$a(f)$	1.001
	t_{th}	10s
	d_0	87m
	E_{da}	5nJ/bit/ packet
	v	1m/s, 2m/s, ..., 6m/s
	v_{sound}	1500m/s
Packet Parameters	p	500bits
	r	50kbps

Then the algorithm performance is obtained with the pair scene parameters changing in the second part. Finally, performance comparisons with five other algorithms (L2-ABF [21], LEACH [29], EL-LEACH [33], ERP^{2}R [34], VBF [35]) are demonstrated.

Simulations are implemented in NS-2 [36] with Aqua-Sim [37] simulation package. Aqua-Sim is an underwater network simulation package, specifically for the extension of underwater environment with 3D infrastructure. It adopts the same memory-less channel with physical channel model. The simulation scene is set as a cube monitoring area, whose edges are 500 m long. 100 to 600 nodes are scattered randomly. The coordinates of BS is (0, 0, 0). Detailed simulation settings are list in Table II. Four network performance metrics, i.e., round numbers (network lifetime), average residual energy of nodes, end-to-end delay and number of living nodes are compared.

A. Scene Parameter Selection

In this section, we design simulations to find out the best algorithm parameter (the range of communication) with different number of nodes and length of SC.

In order to select an optimal value of range of communication as maximum capacity of counter records in this simulation, we change scene parameters (number of nodes and length of SC) to observe the average residual energy with different values of communication range. Simulation rounds are 100 rounds. Besides, λ and μ are set to 1. Simulation results are shown in Fig. 5.

As shown in Fig. 5, average residual energy varies when the value of communication range changes. The improper value of communication range will affect the quality of input of EGRC. Simulation results show that communication range should be set to 7 except when the number of node changes. Under that circumstance, communication range should be from 6 to 8.

B. Algorithm Performance With Pair Scene Parameters Changing

In this section, we set simulations to select two optimal scene parameters: the length of SC and the number of nodes. In this simulation, the number of nodes is set to 100, 200, 300, 400, 500, 600, and length of SC is set to 10 m, 20 m, 30 m, 40 m, 50 m, respectively. Besides λ and μ are set to 1. Simulation round is 100 rounds, and the communication range is set to 70 m. Simulation results are shown in Fig. 6.

It can be seen from Fig. 6 (a) to (d) that both average residual energy and network lifetime increase and end-to-end delay decreases with the augment of number of nodes and the increasement of SC's length in a range. In addition, the increasing range of network lifetime is as much as the range of average residual energy and the decreasing range of end-to-end delay with the augment of nodes' number. Accordingly, the optimal number of nodes is set as a relative small value 500, and the length of SC is set to 30 m.

C. Algorithm Performance With λ and μ Changing

In this section, we set simulations to observe the performance of EGRC with the changing of λ and μ. There are 400 nodes deployed randomly at speed 3m/s in network. The radio communication range is set as 70 m, the simulation rounds is set to 100, and the length of SC is set to 30 m. What's more, λ is set to 1, 2, 4, 6, 8, so as to μ. Simulation results are shown in Fig. 7.

As shown in Fig. 7 (a), with the value of λ increasing, the average residual energy increases. However, the average residual energy increases slowly when the value of μ is equal to or bigger than λ. In Fig. 7 (b), end-to-end delay of EGRC is the lowest when the value of μ is 8 and value of λ is 1, which means end-to-end delay takes up high proportion in $Vertex(i)$.

D. Algorithm Comparisons

In this section, we set two groups of simulations. The proposed EGRC algorithm is compared with LEACH, EL-LEACH and ERP^{2}R to observe the change of three performance metrics with different values of simulation rounds and different number of nodes. Then, EGRC is compared with VBF and L2-ABF to observe the change of three performance metrics with different speed of nodes.

(1) There are 400 nodes deployed randomly at speed 3m/s in network. The radio communication range is set as 70 m. Simulation round is set to 10, 20, …, 400, respectively. Besides, λ and μ are set to 1. Simulation results are shown in Fig. 8–Fig. 11.

The round numbers changing with three parameters (FND, HND and LND) are plotted in Fig. 8. From this figure, we can easily find the advantage of EGRC compared with LEACH, EL-LEACH and ERP^{2}R. When FND of LEACH is at the 15 rounds, EL-LEACH, EGRC and ERP^{2}R achieve 18 rounds. After 85 rounds, the number of dead nodes of LEACH is at half. While in EGRC, HND is 267 rounds. LEACH stops running after 149 rounds but EGRC can reach 379 rounds.

Fig. 9 shows that the average residual energy of nodes in EGRC always outperforms in LEACH,

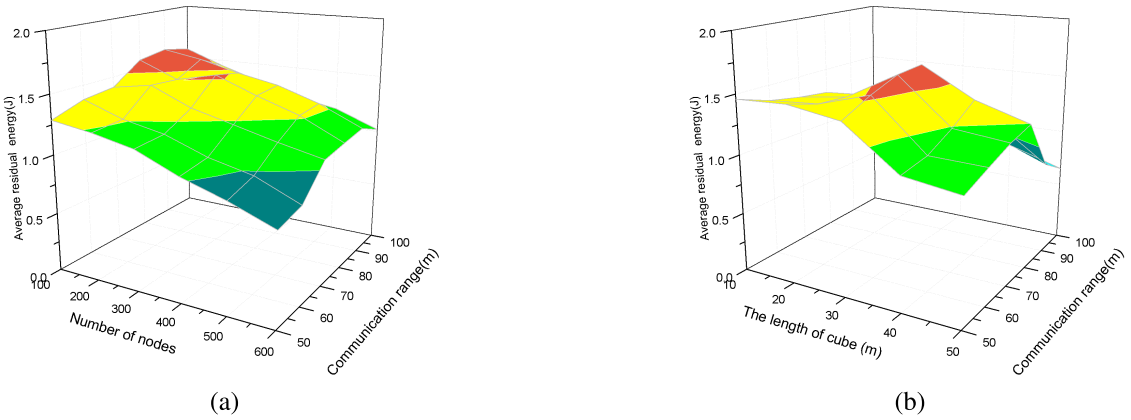

Fig. 5. Scene parameter of communication range. (a) Average residual energy changes with number of node and communication range. (b) Average residual energy changes with length of SC and communication range.

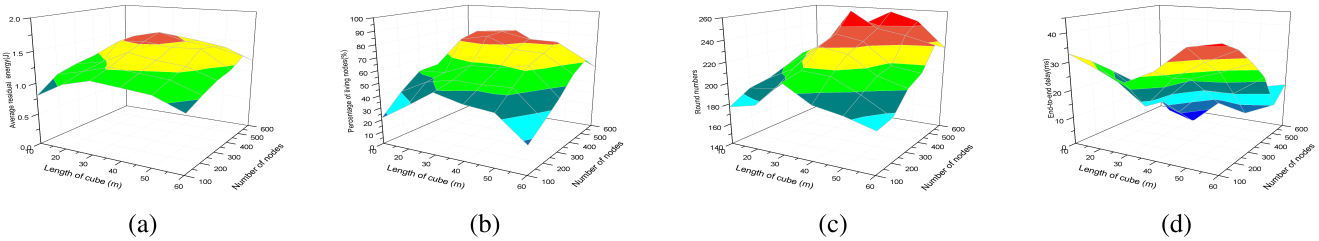

Fig. 6. (a) Average residual energy changes with number of node and length of SC. (b) Percent of living nodes changes with number of node and length of SC. (c) The round changes when a half of nodes are still alive. (d) End-to-end delay with number of node and length of SC.

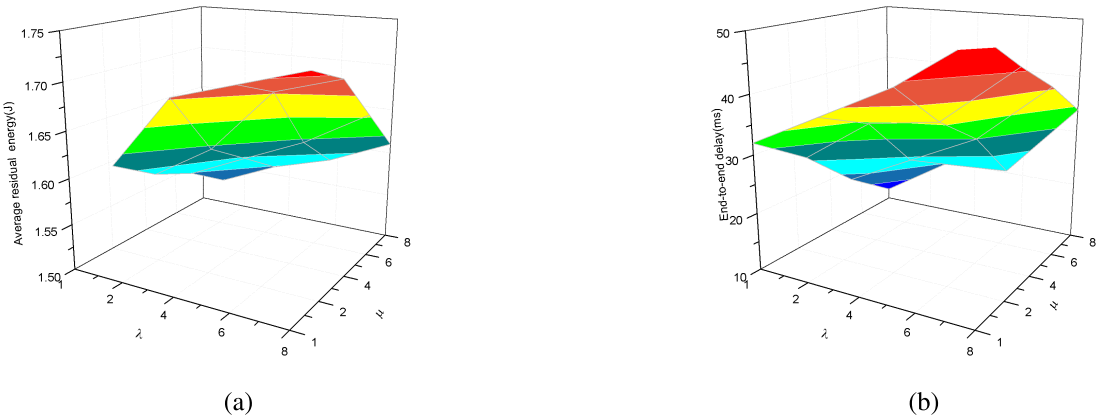

Fig. 7. (a) Average residual energy changes with λ and μ. (b) End-to-end delay changes with λ and μ.

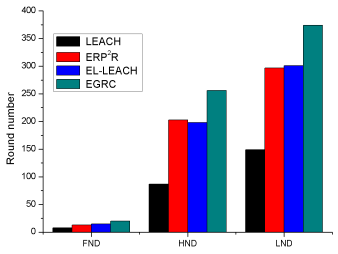

Fig. 8. Number of rounds when different numbers of nodes are dead (FND: the first node dead parameter (the round when the first node dies); HND: half node dead parameter (the round when a half of nodes die); LND: Last node dead parameter (the round when all nodes are dead)).

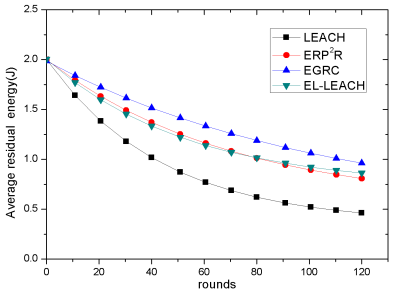

Fig. 9. Average residual energy with different rounds.

EL-LEACH and ERP^{2}R. After 120 rounds, the average residual energy of EGRC is approximately 1.02J, while in EL-LEACH the value is 0.89J, in LEACH the value is 0.46J and in ERP^{2}R is 0.79J, which is almost 1.5 times higher than ERP^{2}R, and twice larger than LEACH. Clearly, it accomplishes better performance

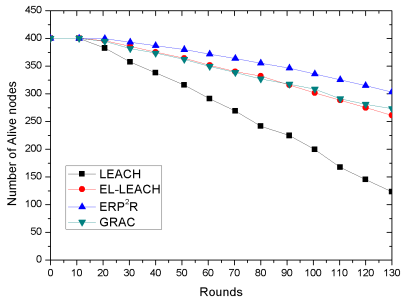

Fig. 10. Number of living nodes with different speed of rounds.

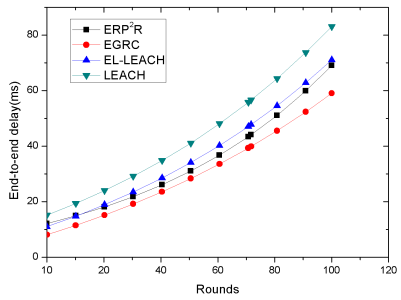

Fig. 11. End-to-end delay with different speed of rounds.

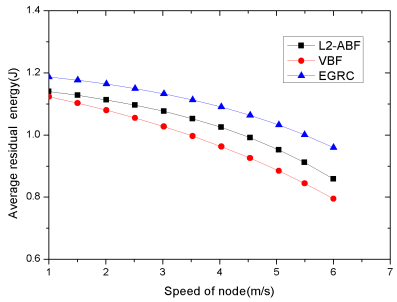

Fig. 12. Average residual energy with different speed of nodes.

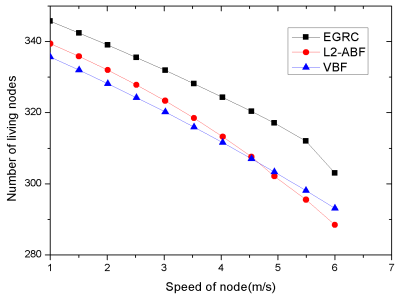

Fig. 13. Number of living nodes with different speed of nodes.

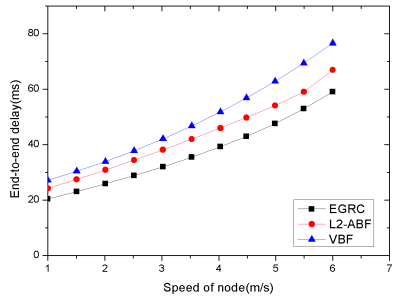

Fig. 14. End-to-end delay with different speed of nodes.

as it consumes less energy, which gives nodes with more residual energy and more opportunity to become a cluster-head node.

In Fig. 10, we set the energy threshold of dead node as 0.01J. From Fig. 10, we can see that the death of first node in EGRC, EL-LEACH and ERP^{2}R is about 18 rounds, while in LEACH the first node dies after 15 rounds. We also find that the number of living nodes of LEACH decreases observably but in EGRC, EL-LEACH and ERP^{2}R, the number of living nodes stays larger and more stable than LEACH. Especially in EGRC, the number of living nodes is the largest and the most stable after 120 rounds. The reason of this advantage in EGRC is that it consumes the least energy in the four algorithms.

From Fig. 11, we can see that the end-to-end delay of EGRC increases more slowly than that of other algorithms with the increament of simulation rounds. What's more, EGRC performs better than LEACH, EL-LEACH and ERP^{2}R in any rounds.

(2) There are 400 nodes deployed randomly in network. The radio communication range is set as 70 m. The speed of nodes is set to 1m/s, 2m/s, 3m/s, 4m/s, 5m/s, 6m/s, respectively. Besides λ and μ are set to 1. We set the simulation rounds as 100 and simulation results are shown in Fig. 12, Fig. 13 and Fig. 14.

In Fig. 12, we can perceive that the average residual energy decreases with the increment of node's speed. That's because when the speed of node increases, it will consume more energy to send information. Even so, EGRC algorithm performs better than VBF and L2-ABF. What's more, the average residual energy of VBF and L2-ABF decreases sharply when the speed of node increases to more than 4m/s, but EGRC performs stable.

In Fig. 13, we also set the energy threshold of dead node as 0.01J. From Fig. 11, we can see that the number of living node differs a lot at different speed of nodes. Especially to VBF and L2-ABF, the number of living nodes decreases sharply with the speed of node increasing. Specifically, when the speed of nodes is 6m/s, the number of living nodes of VBF is about 293, that of L2-ABF is about 288, and that of EGRC is almost 308. Therefore, it is obvious that EGRC has more living nodes than that of VBF and L2-ABF.

Fig. 14 shows that the end-to-end delay of nodes in EGRC always outperforms that of VBF and L2-ABF. When the speed of node is 6m/s, the end-to-end delay of VBF is about 76ms, that of L2-ABF is almost 66ms, and that of EGRC is about 54ms, which means EGRC performs better than VBF and L2-ABF in terms of end-to-end delay.

V. Conclusion and Future Work

In this paper, a new energy-efficient data transmission scheme is proposed, in which the whole 3D network is divided into several SCs and each SC forms a cluster. There is a cluster-head node in each cluster in charge of the data aggregation and transmission of cluster members. A novel algorithm for cluster-head selection is proposed, which selects the node with the highest residual energy and the shortest

TABLE III
LIST OF SYMBOLS IN THE PAPER

Symbols	Description	Section
N	Number of nodes	III-A
b	Length of big cube' edge	III-A
k	Length of SC' edge	III-A
c	Communication range of node	III-A
(x,y,z)	Coordinates of node in three dimension	III-A
$G_i(m,n,h)$	SC identifier of node in three dimension (m, n, h)	III-A
$D_{i,j}$	Distance between node i and node j	III-A
E_{da}	Energy consumption for node to aggregate data	III-A
Cluster-List []	Array of cluster members	III-A
E_{init}	Initial energy of the node	III-B
E_{res}	Residual energy of the node	III-B
E_{tx}	Energy consumption for node to transmit data packets	III-B
E_{Rx}	Energy consumption for node to receive data packets	III-B
l	Number of bits of a packet	III-B
d	distance between transmitter and receiver	III-B
d_0	Threshold distance	III-B
ε_{elec}	Radio dissipation of running transmitter and receiver circuitry	III-B
ε_{fs}	Transmit amplifier coefficient of free space	III-B
ε_{mp}	Transmit amplifier coefficient of multipath space	III-B
f	Frequency of acoustic signal	III-B
$a(f)$	Absorption coefficient	III-B
pr_i	Propagation time form node i to j	III-C
a_i	Byte alignment time	III-C
r_i	Data transmission rate	III-C
tr_i	Transmission and reception time	III-C
t_{ij}	Delay from node i to j	III-C
v_{sound}	Speed of acoustic signal in water	III-C
t_{th}	Delay threshold	III-C
p	Packet size	III-C
$D_{G,bs}$	Distance from the SC to BS	III-D
T_i	Length of timer	III-D
$cluster_T$	A tag to cluster task	III-D
Cluster-list[]	An array to store cluster-member nodes	III-D
NCT(i)	Neighbor cluster-head node table of node i	III-D
C_i	An index to decide cluster-head node i	III-D
Vertex(i)	An index to decide the next-hop node i	III-E
RT(i)	Route table of node i	III-E
v	Speed of nodes	III-E
Δ_{ic}^{-}	Maximum decrement of weight *Vertex(i)*	III-E
Δ_{ic}^{+}	Maximum increment of weight *Vertex(i)*	III-E
λ	Parameters to value the importance of energy	III-E
μ	Parameters to value the importance of delay	III-E

distance to base station as a cluster-head node. Furthermore, we present a mechanism for searching for the next-hop node, which is also based on residual energy, distance and end-to-end delay. Simulation results show that EGRC saves more energy and has longer network lifetime in comparison with LEACH, EL-LEACH and ERP^{2}R. What's more, EGRC also performs better than VBF and L2-ABF in energy efficiency, network lifetime and end-to-end delay. Further improvements and verification are needed in the aspects of applying it to industrial plants, EGRC is verified experimentally to be an efficient strategy in leak points prediction of marine oil pipelines.

APPENDIX
GLOSSARY

See Table III.

REFERENCES

[1] I. F. Akyildiz, D. Pompili, and T. Melodia, "Underwater acoustic sensor networks: Research challenges," *Ad Hoc Netw.*, vol. 3, no. 3, pp. 257–279, May 2005.

[2] G. Han, J. Jiang, L. Shu, and M. Guizani, "An attack-resistant trust model based on multidimensional trust metrics in underwater acoustic sensor network," *IEEE Trans. Mobile Comput.*, Feb. 2015, doi: 10.1109/TMC.2015.2402120.

[3] M. Ayaz, I. Baig, A. Abdullah, and I. Faye, "Review: A survey on routing techniques in underwater wireless sensor networks," *J. Netw. Comput. Appl.*, vol. 34, no. 6, pp. 1908–1927, Nov. 2011.

[4] T. Hu and Y. Fei, "QELAR: A machine-learning-based adaptive routing protocol for energy-efficient and lifetime-extended underwater sensor networks," *IEEE Trans. Mobile Comput.*, vol. 9, no. 6, pp. 796–809, Jun. 2010.

[5] F. Yuan, Y. Zhan, and Y. Wang, "Data density correlation degree clustering method for data aggregation in WSN," *IEEE Sensors J.*, vol. 14, no. 4, pp. 1089–1098, Apr. 2014.

[6] H. Lin and H. Uster, "Exact and heuristic algorithms for data-gathering cluster-based wireless sensor network design problem," *IEEE/ACM Trans. Netw.*, vol. 22, no. 3, pp. 903–916, Jun. 2014.

[7] D. C. Hoang, R. Kumar, and S. K. Panda, "Realisation of a cluster-based protocol using fuzzy C-means algorithm for wireless sensor networks," *IET Wireless Sensor Syst.*, vol. 3, no. 3, pp. 163–171, Sep. 2013.

[8] J. Wu, L. Zhang, Y. Bai, and Y. Sun, "Cluster-based consensus time synchronization for wireless sensor networks," *IEEE Sensors J.*, vol. 15, no. 3, pp. 1404–1413, Mar. 2015.

[9] M. Ayaz, A. Abdullah, and L. T. Jung, "Temporary cluster based routing for underwater wireless sensor networks," in *Proc. IEEE Int. Symp. Inf. Technol. (ITSim)*, vol. 2, Jun. 2010, pp. 1009–1014.

[10] M. C. Domingo and R. Prior, "A distributed clustering scheme for underwater wireless sensor networks," in *Proc. IEEE 18th Int. Symp. Pers., Indoor Mobile Radio Commun. (PIMRC)*, Sep. 2007, pp. 1–5.

[11] K. Ovaliadis, N. Savage, and V. Tsiantos, "A new approach for a better recovery of cluster head nodes in underwater sensor networks," in *Proc. IEEE Int. Conf. Telecommun. Multimedia (TEMU)*, Jul. 2014, pp. 167–172.

[12] N. Goyal, M. Dave, and A. K. Verma, "Fuzzy based clustering and aggregation technique for under water wireless sensor networks," in *Proc. IEEE Int. Conf. Electron. Commun. Syst. (ICECS)*, Feb. 2014, pp. 1–5.

[13] Y. Han, J. Tang, Z. Zhou, M. Xiao, L. Sun, and Q. Wang, "Novel itinerary-based KNN query algorithm leveraging grid division routing in wireless sensor networks of skewness distribution," *Pers. Ubiquitous Comput.*, vol. 18, no. 8, pp. 1989–2001, Dec. 2014.

[14] Y.-P. Chi and H.-P. Chang, "An energy-aware grid-based routing scheme for wireless sensor networks," *Telecommun. Syst.*, vol. 54, no. 4, pp. 405–415, Dec. 2013.

[15] Y. Kim, J. Kim, H. Nam, and S. An, "Hex-grid based routing protocol in wireless sensor networks," in *Proc. IEEE 15th Int. Conf. Comput. Sci. Eng. (CSE)*, Dec. 2012, pp. 683–688.

[16] Y. Ren, N. Yu, X. Guo, and J. Wan, "Cube-scan-based three dimensional localization for large-scale underwater wireless sensor networks," in *Proc. IEEE Int. Syst. Conf. (SysCon)*, Mar. 2012, pp. 1–6.

[17] M. Liu, J. Cao, G. Chen, and X. Wang, "An energy-aware routing protocol in wireless sensor networks," *Sensors*, vol. 9, no. 1, pp. 445–462, 2009.

[18] K. Wang and H. Guo, "An improved routing algorithm based on social link awareness in delay tolerant networks," *Wireless Pers. Commun.*, vol. 75, no. 1, pp. 397–414, Mar. 2014.

[19] W. Jin, M. Tinghuai, C. Jinsung, and L. Sungoung, "An energy efficient and load balancing routing algorithm for wireless sensor networks," *Comput. Sci. Inf. Syst.*, vol. 8, no. 4, pp. 991–1007, 2011.

[20] K. Wang and M. Wu, "Cooperative communications based on trust model for mobile ad hoc networks," *IET Inf. Secur.*, vol. 4, no. 2, pp. 68–79, Jun. 2010.

[21] T. Ali, L. T. Jung, and I. Faye, "End-to-end delay and energy efficient routing protocol for underwater wireless sensor networks," *Wireless Pers. Commun.*, vol. 79, no. 1, pp. 339–361, Nov. 2014.

[22] S. Zhang, D. Li, and J. Chen, "A link-state based adaptive feedback routing for underwater acoustic sensor networks," *IEEE Sensors J.*, vol. 13, no. 11, pp. 4402–4412, Nov. 2013.

[23] S. Gopi, K. Govindan, D. Chander, U. B. Desai, and S. N. Merchant, "E-PULRP: Energy optimized path unaware layered routing protocol for underwater sensor networks," *IEEE Trans. Wireless Commun.*, vol. 9, no. 11, pp. 3391–3401, Nov. 2010.

[24] J. Cao, J. Dou, Z. Guo, S. Dong, and H. Xu, "ELT: Energy-level-based hybrid transmission in underwater sensor acoustic networks," in *Proc. 9th IEEE Int. Conf. Mobile Ad-Hoc Sensor Netw. (MSN)*, Dec. 2013, pp. 133–139.
[25] G. Han, J. Jiang, L. Shu, Y. Xu, and F. Wang, "Localization algorithms of underwater wireless sensor networks: A survey," *Sensors*, vol. 12, no. 2, pp. 2026–2061, 2012.
[26] G. Han, C. Zhang, L. Shu, and J. J. P. C. Rodrigues, "Impacts of deployment strategies on localization performance in underwater acoustic sensor networks," *IEEE Trans. Ind. Electron.*, vol. 62, no. 3, pp. 1725–1733, Mar. 2015.
[27] L. Shu, Z. Yuan, T. Hara, L. Wang, and Y. Zhang, "Impacts of duty-cycle on TPGF geographical multipath routing in wireless sensor networks," in *Proc. 18th Int. Workshop Quality Service (IWQoS)*, Jun. 2010, pp. 1–2.
[28] S. Nath and P. B. Gibbons, "Communicating via fireflies: Geographic routing on duty-cycled sensors," in *Proc. 6th ACM Int. Conf. Inf. Process. Sensor Netw.*, 2007, pp. 440–449.
[29] W. R. Heinzelman, A. Chandrakasan, and H. Balakrishnan, "Energy-efficient communication protocol for wireless microsensor networks," in *Proc. IEEE 33rd Annu. Hawaii Int. Conf. Syst. Sci. (HICSS)*, Jan. 2000, pp. 8020–8030.
[30] M. Stojanovic, "On the relationship between capacity and distance in an underwater acoustic communication channel," *ACM SIGMOBILE Mobile Comput. Commun. Rev.*, vol. 11, no. 4, pp. 34–43, Oct. 2007.
[31] W. H. Thorp, "Analytic description of the low-frequency attenuation coefficient," *J. Acoust. Soc. Amer.*, vol. 42, no. 1, p. 270, 1967.
[32] A. A. Syed and J. Heidemann, "Time synchronization for high latency acoustic networks," in *Proc. 25th IEEE Int. Conf. Comput. Commun. (INFOCOM)*, Apr. 2006, pp. 1–12.
[33] T. N. Quynh, K.-H. Phung, and H. V. Quoc, "Improvement of energy consumption and load balance for LEACH in wireless sensors networks," in *Proc. Int. Conf. ICT Converg. (ICTC)*, Oct. 2012, pp. 583–588.
[34] A. Wahid, S. Lee, and D. Kim, "An energy-efficient routing protocol for UWSNs using physical distance and residual energy," in *Proc. IEEE-Spain OCEANS*, Jun. 2011, pp. 1–6.
[35] P. Xie, J.-H. Cui, and L. Lao, "VBF: Vector-based forwarding protocol for underwater sensor networks," in *Networking Technologies, Services, and Protocols; Performance of Computer and Communication Networks; Mobile and Wireless Communications Systems* (Lecture Notes in Computer Science), vol. 3976. Berlin, Germany: Springer-Verlag, 2006, pp. 1216–1221.
[36] *NS-2: Network Simulator*. [Online]. Available: http://www.isi.edu/nsnam/ns, accessed Nov. 2014.
[37] P. Xie *et al.*, "Aqua-Sim: An NS-2 based simulator for underwater sensor networks," in *Proc. IEEE/MTS OCEANS*, Oct. 2009, pp. 1–7.

Kun Wang (M'13) received the Ph.D. degree from the School of Computer, Nanjing University of Posts and Telecommunications, in 2009. He was a Post-Doctoral Fellow with the Electrical Engineering Department, University of California, Los Angeles (UCLA), CA, USA, from 2013 to 2014. He is currently an Associate Professor with the School of Internet of Things, Nanjing University of Posts and Telecommunications, Nanjing, China. He has authored over 50 papers in related international conferences and journals, including the *IEEE Communications Magazine*, the IEEE Globecom Conference 2013, and the IEEE International Conference on Communications in 2014. His current research interests include wireless sensor networks, delay tolerant networks, stream computing, ubiquitous computing, mobile cloud computing and information security technologies. He is a member of the Association for Computing Machinery.

Hui Gao is currently pursuing the master's degree in logistics engineering at the Nanjing University of Posts and Telecommunications. Her current research interests include wireless sensor networks and underwater acoustic sensor networks.

Xiaoling Xu received the M.S. degree in control theory and control engineering from Henan Polytechnic University, in 2008. She has served for five years as a Teacher of Measurement Technology and Instrument Specialty with the Guangdong University of Petrochemical Technology. Her current research interests are wireless sensor networks and intelligent control.

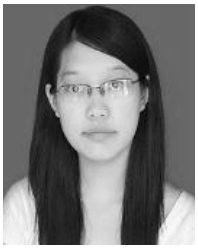

Jinfang Jiang received the B.S. degree in information and communication engineering from Hohai University, China, in 2009. She is currently pursuing the Ph.D. degree at the Department of Information and Communication System, Hohai University. Her current research interests are security and localization for sensor networks.

Dong Yue received the Ph.D. degree from the South China University of Technology, Guangzhou, China, in 1995. He is currently a Professor and Dean of the Institute of Advanced Technology with the Nanjing University of Posts and Telecommunications, and also a Changjiang Professor with the Department of Control Science and Engineering, Huazhong University of Science and Technology. He is currently an Associate Editor of the IEEE Control Systems Society Conference Editorial Board and also an Associate Editor of the *International Journal of Systems Science*. He has authored over 100 papers in international journals, domestic journals, and international conferences. His research interests include analysis and synthesis of networked control systems, multiagent systems, optimal control of power systems, and Internet of things.